Biochemistry

pubs.acs.org/biochemistry Article

Natural and Synthetic Suppressor Mutations Defy Stability−Activity Tradeoffs

Sonya Lee,[#] Cynthia N. Okoye,[#] Devin Biesbrock, Emily C. Harris, Katelyn F. Miyasaki, Ryan G. Rilinger, Megalan Tso, and Kathryn M. Hart*

Cite This: *Biochemistry* 2022, 61, 398−407 Read Online

ACCESS | Metrics & More | Article Recommendations | Supporting Information

ABSTRACT: Thermodynamic stability represents one important constraint on protein evolution, but the molecular basis for how mutations that change stability impact fitness remains unclear. Here, we demonstrate that a prevalent global suppressor mutation in TEM β-lactamase, M182T, increases fitness by reducing proteolysis *in vivo*. We also show that a synthetic mutation, M182S, can act as a global suppressor and suggest that its absence from natural populations is due to genetic inaccessibility rather than fundamental differences in the protein's stability or activity.

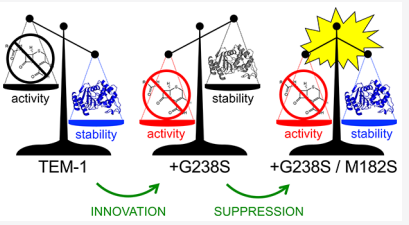

INTRODUCTION

Enzymes involved in antibiotic resistance are subject to strong selective pressures due to the prevalence of antibiotics in clinical and agricultural environments. Although these enzymes first evolved to combat naturally occurring antibiotics (e.g., penicillin) and predate modern antibiotic usage,[1] they can quickly evolve activity against synthetic antibiotics designed by humans. TEM β-lactamase, for example, is a family of enzymes that catalyze the hydrolysis of β-lactam antibiotics and represents one of the most prevalent mechanisms of microbial resistance observed in clinical settings.[2] The first variant identified, TEM-1, confers resistance to penicillins but not later-generation cephalosporins like cefotaxime; however, a single missense mutation in TEM can increase resistance to cefotaxime by several orders of magnitude.[3] Currently, over 200 clinical variants of TEM have been identified, and they differ in sequence at anywhere from one to a dozen positions that occur throughout the three-dimensional structure.[4] While these differences in sequence do little to change the native structure of the enzyme, they do have an impact on thermodynamic stability, activity, and organismal fitness. For instance, TEM-52, which differs from TEM-1 at three positions (out of 263 total), has a Cα RMSD of 0.99 Å with TEM-1 (Figure 1) but increases cefotaxime resistance by 500-fold.[5] One of the substitutions in this variant, G238S, has been shown to exhibit a so-called stability−activity tradeoff:[6] it increases activity against cefotaxime by 100-fold but decreases thermostability of the enzyme by 5 °C.[6]

Stability−activity tradeoffs are a well-established phenomenon in molecular evolution. Missense mutations that alter a protein's function can be selected if they increase organismal fitness, but because change-of-function substitutions often occur at positions buried in the protein's structure, they also tend to reduce protein stability. In the ribonuclease barnase, for example, substituting acidic residues with basic residues in the active site relieves electrostatic strain but reduces activity.[7] Similarly, optimizing interactions between side chains in the active site of T4 lysozyme comes at the cost of binding the reaction's transition state.[8] In both cases, the protein's stability is enhanced whereas catalysis suffers. When an enzyme evolves new functions, the inverse is likely to occur, and the enzyme may become destabilized. From a thermodynamic perspective, stability reflects the population of folded, functional molecules, so at some threshold, destabilization will exact a fitness cost. In this way, thermodynamic stability represents one important constraint on protein evolution, and stabilizing mutations are important for evolutionary innovation. Indeed, it has been observed that stabilizing mutations enhance evolvability,[9,10] or the ability of a protein to undergo adaptive evolution in both

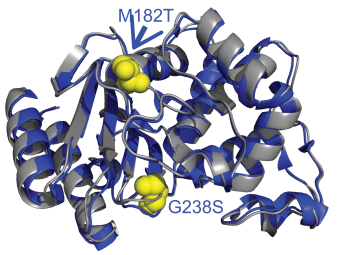

Figure 1. Overlay of TEM-1 (PDB 1BTL, shown in gray) and the extended spectrum variant TEM-52 (PDB 1HTZ, shown in blue). Position 238 lines the active site and is separated from position 182 by ~18 Å (shown in yellow spheres).

Received: December 16, 2021
Revised: January 26, 2022
Published: February 10, 2022

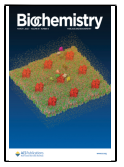

https://doi.org/10.1021/acs.biochem.1c00805
Biochemistry 2022, 61, 398−407

natural settings[11] and laboratory evolution experiments.[12] By characterizing mutations that restore stability to evolving proteins—and identifying new ones—we can better understand the nature of physical constraints on molecular evolution and identify the specific molecular mechanisms at play.

Understanding the precise relationship between TEM stability and organismal fitness is complicated by the fact that TEM populates a partially folded intermediate at equilibrium. Intermediates are common—particularly in multidomain proteins—but their role in protein evolution is not well understood. It has been suggested that intermediates exact a fitness cost due to their tendency to aggregate,[13,14] but numerous studies have demonstrated that intermediates can be eliminated with minor sequence changes,[15−18] implying that they are not necessarily selected against. We sought to approach this issue by determining whether the intermediate—and specifically its stability—was important in the evolution of β-lactamase. Because we can detect and measure the stabilities of TEM's native and intermediate states using a combination of circular dichroism (CD) and intrinsic fluorescence, we can determine the effects of mutations on both and draw connections to organismal fitness.

G238S is also found in clinical settings in combination with another substitution, M182T, which restores stability and acts as a suppressor of misfolding and aggregation.[19] A previous work demonstrated that M182T stabilizes the native state but does not impact the stability of an equilibrium intermediate.[20] M182S is a synthetic stabilizing mutation in TEM that has not been observed in nature. Both M182T and M182S stabilize the native state (N) of TEM by 3−4 kcal/mol but do not affect the stability of a partially unfolded intermediate (I) present at equilibrium.[20] Because wild type's global stability, defined as the free energy difference between N and the unfolded state (U), is already quite high (ΔG_{NU} = 14.8 kcal/mol), it is unclear whether additional stabilization offers any fitness advantage. Indeed, while M182T is a common mutation in extended-spectrum β-lactamases, it is most often observed in combination with other mutations rather than on its own. This is a classic example of evolution reconciling stability−activity tradeoffs: primary mutations, like G238S, increase activity against new antibiotics but tend to be destabilizing; and secondary mutations, like M182T, restore stability but may not offer much fitness advantage on their own.[6]

Here, we examine M182T and M182S alone and in combination with G238S to determine whether there are fundamental differences between clinical versus synthetic mutations and to determine the extent to which stability and activity contribute to fitness.

MATERIALS AND METHODS

Protein Expression and Purification. Overexpression plasmids were constructed by subcloning TEM-1 into a pET24 vector (Life Technologies) with its native export signal sequence replaced by the OmpA signal sequence to maximize export efficiency.[21] Variants were constructed via site-directed mutagenesis and verified by DNA sequencing. Plasmids were transformed into BL21(DE3) cells (Life Technologies) for expression under a T7 promoter control. Cells were induced with 1 mM IPTG at OD = 0.6 and grown at 18 °C for 15 h before harvesting.

TEM β-lactamases were isolated from the periplasmic fraction using osmotic shock lysis: Cells were resuspended in 30 mM Tris-Cl, pH 8, and 20% sucrose and stirred for 10 min at room temperature. After centrifugation, the pellet was resuspended in ice-cold 5 mM $MgSO_4$ and stirred for 10 min at 4 °C. After centrifugation, the supernatant was dialyzed against 20 mM sodium acetate, pH 5.5, and purified using cation exchange chromatography (HiTrap Capto S column, GE Healthcare). All variants eluted between 10 and 20% NaCl. Proteins were concentrated, dialyzed in storage buffer (20 mM Tris, pH 8.0), and final concentrations were measured in Edelhoch buffer using calculated extinction coefficients based on the number of tryptophans, tyrosines, and disulfide bonds.[22]

Enzyme Activity Measurements. Kinetic parameters of the β-lactamase variants with benzylpenicillin, $\varepsilon_{232\ nm} = -1096\ M^{-1}\ cm^{-1}$, and cefotaxime, $\varepsilon_{265\ nm} = -6643\ M^{-1}\ cm^{-1}$, were determined using an Agilent Cary 60 UV−Vis spectrophotometer. The kinetic reaction was carried out in a 600 μL total volume with activity buffer (50 mM potassium phosphate, pH 7.0, 10% glycerol) and a final enzyme concentration of 2−200 nM at 25 °C. To obtain the kinetic parameters K_m and k_{cat}, the data were fit by the Michaelis−Menten equation.

Protein Stability Measurements. Individual samples with variable concentrations of urea were prepared in 25 mM sodium phosphate pH 6.6 with ∼0.03 mg/mL protein. Samples were left to equilibrate overnight at room temperature before analysis by CD and fluorescence spectrometry (1 cm cuvette, 25 °C). CD data was collected using a Jasco J-815 CD Spectrometer or an Applied Photophysics Chirascan V100 Spectrometer. CD was monitored at 222 nm and averaged over 1 min after 1 min of equilibration at 25 °C in a cell holder. Fluorescence was collected using a PerkinElmer LS 55 Fluorescence Spectrometer or Applied Photophysics Chirascan CCD Fluorometer, exciting at 280 nm and detecting emission at 340 nm.

Fluorescence data were fit by a two-state model (N-to-I) using the linear extrapolation method to determine ΔG_{NI} and m_{NI} in the absence of urea (eq 1).[23] CD data were fit by a three-state model (U-to-I-to-N) constrained by the average ΔG_{NI} and m_{NI} values from triplicate fluorescence melts to determine ΔG_{IU} and m_{IU} (eq 2).

$$\text{total fluorescence}(f) = \frac{f_N + f_I\, e^{-(\Delta G_{NI} - m_{NI}[\text{urea}])/RT}}{1 + e^{-(\Delta G_{NI} - m_{NI}[\text{urea}])/RT}} \quad (1)$$

$$\text{total CD}(\Theta) = \frac{\Theta_N + \Theta_I\, e^{-(\Delta G_{NI} - m_{NI}[\text{urea}])/RT} + \Theta_U\, e^{-(\Delta G_{NI} + \Delta G_{IU} + [\text{urea}](m_{NI} + m_{IU}))/RT}}{1 + e^{-(\Delta G_{NI} - m_{NI}[\text{urea}])/RT} + e^{-(\Delta G_{NI} + \Delta G_{IU} - [\text{urea}](m_{NI} + m_{IU}))/RT}} \quad (2)$$

where f_N and f_I are the fluorescence values of the native and intermediate states, respectively, fit as lines; Θ_N, Θ_I, and Θ_U are the CD signals of the native, intermediate, and unfolded states, respectively, fit as lines; ΔG_{NI} is the free energy change and m_{NI} is the m-value of the N-to-I transition; and ΔG_{IU} and m_{IU} are the free energy and m-value of the I-to-U transition.

Pulse Proteolysis. Pulse proteolysis experiments were performed according to published protocols.[24] Briefly, 100 μL samples of 0.5 mg/mL protein in buffer (20 mM Tris-Cl pH 8, 10 mM $CaCl_2$) were prepared with varying concentrations of urea and allowed to equilibrate at room temperature overnight. To initiate proteolysis, 0.2 mg/mL thermolysin (Promega) was added to each sample and briefly vortexed. After 1 min, the reaction mixtures were quenched with 10 mM EDTA, diluted with loading buffer, and separated using SDS-PAGE (Any kD Mini-Protean TGX gel, Bio-Rad). It was verified that folded protein was not degraded during the 1 min pulse by performing a

https://doi.org/10.1021/acs.biochem.1c00805
Biochemistry 2022, 61, 398−407

time course experiment.[24] Gels were stained with SYPRO Red Stain (Lonza) and imaged using a G:box Chemi XT4 system (Syngene). Bands were quantified using ImageJ.

Immunoblotting and Quantification. Cell cultures were grown overnight in 50 mL of Mueller-Hinton II media and kanamycin with the addition of 1 mM IPTG for overexpression strains. To prepare whole cell samples, cells from 500 μL of culture (OD_{600} = 3−4) were diluted with 40−200 μL of loading buffer, boiled, and spun before loading the supernatant in the gel. To prepare periplasmic samples, cell pellets from 50 mL cultures were first equilibrated in 2.0 mL of 20% sucrose buffer (30 mM Tris-Cl pH 8) containing 1× ProBlock Gold Bacterial cocktail (GoldBio) and 1 mM EDTA. Then, the outer membranes were lysed via osmotic shock in 2.0 mL of ice-cold 5 mM $MgSO_4$ containing 1× ProBlock Gold Bacterial cocktail and centrifuged. Soluble protein samples were made from the resulting supernatant. The cell pellets were resuspended in 6 M urea buffer (30 mM Tris−HCl pH 8), spun, and insoluble protein samples were made from the resulting supernatant. All samples were boiled for 3 min at 100 °C and centrifuged prior to loading the supernatant in the gel.

Following separation by SDS-PAGE (Any kD Mini-Protean TGX gel, Bio-Rad), proteins were transferred to PVDF membranes (Amersham Life Science) for 12 to 16 h at 30 V. Membranes were incubated with monoclonal mouse anti-β-lactamase primary antibody (1:2000 dilution; Invitrogen MA1-20370) for 45 min followed by a rabbit anti-mouse horseradish peroxidase conjugated secondary antibody (1,10,000 dilution; Invitrogen 31457) for 45 min. Binding was detected by using an ECL substrate kit (Thermo Scientific Pierce) according to the manufacturer's instructions and imaged using a G:box Chemi XT4 system (Syngene). Quantification of bands was performed using ImageJ and normalized to internal standards of purified TEM.

Minimum Inhibitory Concentration (MIC) Determination. *Escherichia coli* strains containing plasmids with various β-lactamase genes were grown overnight at 37 °C in LB broth with kanamycin. The antibacterial activity of the compounds was determined by measuring their minimum inhibitory concentrations (MIC) using the broth microdilution method according to the Clinical and Laboratory Standards Institute (CLSI, formerly the NCCLS) guidelines. Each well of a 96-well microtiter plate was filled with 50 μL of sterile Mueller Hinton II cation-adjusted media broth. A total of 50 μL of the compound solution in media was added to the first column of the microtiter plate and 2-fold serial dilutions were made down each row of the plate. A total of 50 μL of bacterial inoculum from overnight LB cultures in minimal media (5×10^5 CFU/mL) was then added to each well, giving a total volume of 100 μL minimal media/well and a compound concentration gradient of 48,000−23 μM (BP) or 288−0.035 μM (CFX). The plate was incubated at 37 °C for 16−18 h, and then, each well was examined for bacterial growth. The MIC was recorded as the lowest compound concentration required to inhibit 90% of bacterial growth as verified by the turbidity of the culture media relative to a row of wells filled with a water standard. Water and chloramphenicol were included as controls in each plate.

Relative Fitness Determination. The native expression plasmids used for fitness competition assays were derived from pBR322, which contains *bla*, and constructed via Gibson assembly to include Kan^R and mCherry genes. Missense mutations were introduced into *bla* and mCherry by site-directed mutagenesis. Two plasmids per *bla* variant were constructed: one with wild-type mCherry and one with Y72L, which eliminates its fluorescence.[25] Heat shock transformation into *E. coli* DH5α (Intact Genomics) was used to construct strains for fitness competition assays. The two strains to be co-cultured were grown separately overnight at 37 °C with shaking at 225 rpm to saturation in LB with 50 μg/L kan. The cultures were then diluted and combined 1:1 in 10 mL of LB with kan to a final $OD_{600\ nm}$ = 0.02 and grown at 37 °C with shaking. Relative fitnesses remained constant from 16 to 48 h, so 16−18 h of growth was used. Bacterial populations were monitored by plating co-culture dilutions on LB + kan agar plates, fluorescence imaging, counting both fluorescent and non-fluorescent colonies, and back calculating the co-culture populations. Plate images were taken with a G:box Chemi XT4 system (Syngene) using a green LED light and filter 605 nm with 6 × 6 (2MP) binning and 8−10 s exposure. All the colonies on the bright field and fluorescent images were counted by hand. Using the colony and the dilution factors for the pre- and post-competition cultures, the number of cells in the culture before and after competitions could be determined and used to calculate the relative fitness of each strain. The relative fitness was calculated according to eq 3.

RESULTS AND DISCUSSION

M182T and M182S Increase Native State Stability. To determine whether M182S restores stability to G238S in a similar manner to M182T, we measured the stabilities of TEM variants containing G238S, M182T, and M182S substitutions both in isolation and in combination (G238S/M182T and G238S/M182S). Previous studies used melting temperatures as a proxy for thermodynamic stability,[6] but because TEM appears to be a two-state in these experiments, it is impossible to attribute changes in stability to N versus I. This is an important distinction because global stability may not be the most relevant when considering fitness impacts. For instance, the native state stability relative to the intermediate may be more relevant than its stability relative to a totally unfolded state since like unfolded states, partially folded states are not active enzymes and may be prone to aggregation and/or proteolysis.

Using urea-induced denaturation of TEM variants detected by both intrinsic fluorescence and CD, we can distinguish impacts on the N-to-I transition from the I-to-U transition (Figure 2). By CD, I is distinct from both N and U, retaining about 75% of the native state's secondary structure. By intrinsic fluorescence, I is indistinguishable from U, presumably due to quenching of tryptophans buried in N but solvent-exposed in I and U. Having distinct probes that are sensitive to each transition allows us to confidently assign ΔG and m-values. It is difficult to determine these values otherwise since the number of parameters results in overfitting the data. Specifically, we can fit the fluorescence data by a two-state model to determine the ΔG and m-values for the N-to-I transition (ΔG_{NI} and m_{NI}). Then, we can fix these parameters in a three-state fit of the CD data to determine ΔG_{IU} and m_{IU} (see the Materials and Methods). The global parameters (ΔG_{NU} and m_{NU}) are the sum of the individual transitions.

Dominant stability effects for all individual substitutions tested are on the native state—not intermediate—stabilities. G238S destabilizes N relative to I by 2.4 kcal/mol, and M182T and M182S stabilize N relative to I by 3.9 and 4.5 kcal/mol, respectively. When combined with G238S, both M182T and M182S fully restore the stability of N (Table 1). The similarities between M182T and M182S in isolation and in combination

https://doi.org/10.1021/acs.biochem.1c00805
Biochemistry 2022, 61, 398−407

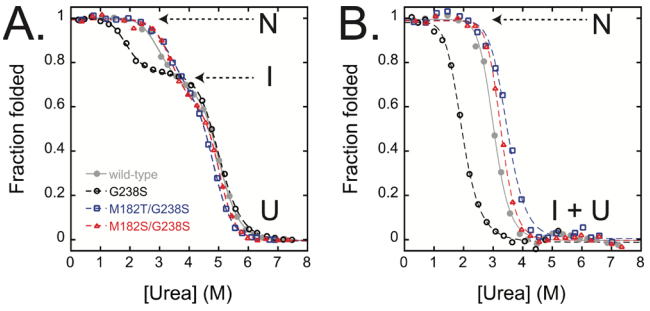

Figure 2. Denaturant melts of TEM variants as detected by (A) CD and (B) intrinsic fluorescence. At least three states are present at equilibrium as indicated by CD, but only two are detectable by fluorescence. Because the intermediate and unfolded states have the same fluorescence signal, these melts highlight the N-to-I transition. All substitutions studied impact only this transition, which means that they impact the native state stability but not stability of the intermediate. Wild-type data appear in gray, closed circles, G238S in black, open circles, G238S/M182T in blue, open squares, and G238S/M182S in red, open triangles.

with the naturally occurring primary mutation G238S are perhaps unsurprising given their chemical and structural similarities. Computational modeling suggests that they form N-capping hydrogen bonds in a helix important to native state stability, and both assume rotamer conformations that stabilize the helix.[20] These features are both crucial components to the mechanism, as helix capping alone by M182N is not stabilizing.[20]

We were surprised to find that the stability effects are not additive given that positions 182 and 238 are ∼18 Å apart in physical space in the crystal structures (Figure 1). Specifically, the mutations exhibit negative epistasis with regard to stability since the double mutants are less stable than the sum of their $\Delta\Delta G_{NI}$s. It is not clear why G238S diminishes the ability of M182T or M182S to stabilize N; in fact, it is not clear why the G238S substitution is destabilizing in the first place. One possibility is that G238S is destabilizing for the same reason that it increases activity—namely, that it pins down the Ω-loop via a hydrogen-bonding interaction with Asn170.[26] The Ω-loop is a highly conserved part of the active site and demonstrates high mobility. G238S restricts its motion, leading to reduced conformational heterogeneity of the native ensemble.[26] Reducing entropy of the native state would be an unusual, though not unprecedented,[27] mechanism of destabilization. Indeed, Gly → Xaa substitutions are typically considered a stabilization strategy due to reduction in the configuration entropy of the unfolded state,[28] but this only holds if the glycine is more constrained in N than in U, which may not be the case here. M182T has also been found to restrict the mobility of the Ω-loop,[29] so this shared effect could be the source of epistasis.

Regardless of the specific molecular mechanisms at play, we observe no differences between the clinical and synthetic mutations by this metric, as both are stabilizing alone and in combination with G238S. We next turned to *in vivo* assays to determine whether any phenotypic differences could be detected.

M182T and M182S Increase Protein Abundance. To determine whether changes in stability have an impact on cellular contexts, we performed quantitative immunoblotting experiments to measure the abundance of the TEM variants in K-12 and B strain *E. coli* (Table 2 and Figure 3). In Gram-negative bacteria, TEM is exported to the periplasm where it degrades antibiotics, targeting the cell-wall synthesis.[30] This process is mediated by a 23-residue signal peptide, or export sequence, that is cleaved during translocation to generate the active enzyme.[31] We evaluated two constructs, varying in levels of expression and export to the periplasm. The first design (overexpression strain) positions the *bla* gene downstream of an IPTG-inducible T7 promoter and contains an artificial export tag from OmpA that is properly processed to generate mature protein.[21] The second design (native expression strain) is a modified pBR322 vector containing a native promoter and export sequence that originated from an ampicillin-resistant R plasmid.[32,33] The first design was evaluated in a B strain, specifically the BL21 (DE3) strain, to facilitate the recognition of the non-native T7 promoter, and the latter in the K-12 strain DH5α.

All variants, including wild-type, express solubly in the periplasm and insolubly in inclusion bodies. Only the soluble, periplasmic protein contributes to antibiotic resistance since insoluble protein aggregates in an inactive form in both the cytoplasm and periplasm.[34] Overall, wild-type TEM abundance is higher in the overexpression strain by ∼20-fold, but the percentage of soluble protein is higher in the strain with native expression, suggesting that proper processing and/or translocation cannot keep up with the synthesis when overexpressed.

Several themes emerge from the immunoblotting experiments. First, G238S reduces the amount of soluble protein relative to the wild type. Second, M182T and M182S increase TEM abundance for both soluble, periplasmic protein and insoluble protein. Last, the increased abundance occurs to similar extents whether in the wild-type or G238S background. We discuss each of these observations below.

Soluble G238S is less abundant than the wild type by ∼5-fold in the overexpression strain and is undetectable under native expression. Interestingly, insoluble G238S levels are comparable to that of the wild type, suggesting that the observed reduction in

Table 1. Stabilities of TEM Variants

	N-to-I transition[a]		I-to-U transition[b]		global stability	
	ΔG_{NI} (kcal mol^{-1})[c]	m_{NI} (kcal mol^{-1} M^{-1})[c]	ΔG_{IU} (kcal mol^{-1})[c]	m_{IU} (kcal mol^{-1} M^{-1})[c]	ΔG_{NU} (kcal mol^{-1})[c]	m_{NU} (kcal mol^{-1} M^{-1})[c]
wild-type	6.1 ± 0.7	2.1 ± 0.2	8.7 ± 2.0	1.7 ± 0.4	14.8 ± 2.1	3.7 ± 0.4
M182T[d]	10.0 ± 0.6	2.4 ± 0.2	7.8 ± 0.2	1.7, fixed	17.7 ± 0.4	4.1 ± 0.2
M182S[d]	10.6 ± 0.5	2.7 ± 0.1	7.9 ± 0.4	1.7, fixed	18.5 ± 0.5	4.4 ± 0.1
G238S	3.7 ± 0.7	1.9 ± 0.3	8.1 ± 0.8	1.6 ± 0.1	11.9 ± 1.0	3.5 ± 0.3
M182T/G238S	6.1 ± 1.1	1.7 ± 0.3	7.5 ± 3.4	1.6 ± 0.6	13.6 ± 3.6	3.3 ± 0.6
M182S/G238S	6.1 ± 1.3	1.8 ± 0.4	8.2 ± 2.4	1.6 ± 0.5	14.2 ± 2.7	3.5 ± 0.6

[a]Determined by a two-state fit to fluorescence emission at 340 nm. [b]Determined by a three-state fit to the CD signal at 222 nm with constrained ΔG_{NI} and m_{NI} values (see Materials and Methods). [c]Errors are the standard deviations from triplicate measurements. [d]From ref 20.

https://doi.org/10.1021/acs.biochem.1c00805
Biochemistry 2022, 61, 398−407

Table 2. Soluble and Insoluble Protein Abundance in TEM-Expression Strains

		native expression in DH5α				overexpression in BL21 (DE3)			
		protein abundance[b]		MIC (μM)[c]		protein abundance[b]		MIC (μM)[c]	
amino acid substitution	clinical variant	soluble	insoluble	BP	CFX	soluble	insoluble	BP	CFX
wild-type	TEM-1	0.50	0.10	12,000	0.04	6.78	5.67	24,000	0.04
M182T	TEM-135	1.46	0.70	24,000	0.04	12.25	21.28	24,000	0.04
M182S	na[a]	1.18	0.64	24,000	0.04	13.79	16.99	24,000	0.04
G238S	TEM-19	0.00	0.00	12,000	2.25	1.48	7.17	6000	4.5
M182T/G238S	TEM-20	1.41	0.46	12,000	9	37.55	67.19	12,000	72
M182S/G238S	na[a]	0.72	0.42	12,000	9	16.04	47.02	12,000	72

[a]Not applicable. Substitution has not been observed in naturally occurring variants. [b]Abundance based on immunoblotting. Pixels are quantified using ImageJ and expressed relative to Std. 1 (see the Materials and Methods). [c]MICs are the most commonly observed concentrations from triplicate measurements. Error is ± one well, and adjacent wells differ two-fold in concentration.

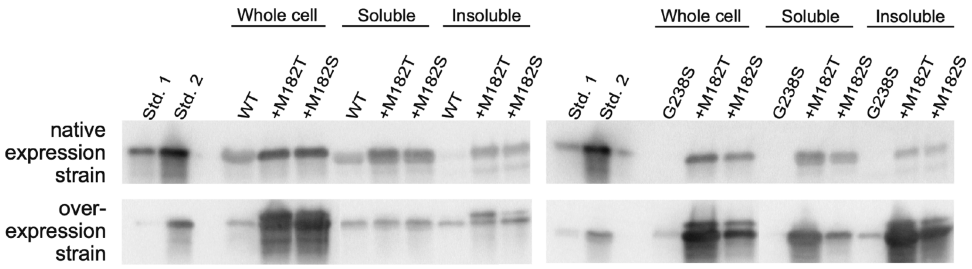

Figure 3. Immunoblots of *E. coli* expressing TEM variants. TEM levels in the periplasm and insoluble fraction were quantified using immunoblotting. Whole cell extracts were prepared by boiling in sample buffer, and periplasmic and insoluble fractions were prepared as described in the Materials and Methods. Purified wild-type TEM was loaded as a standard at two dilutions (Std. 1 and Std. 2). G238S is much less abundant than the wild type, and the presence of M182T or M182S increased abundance in all contexts.

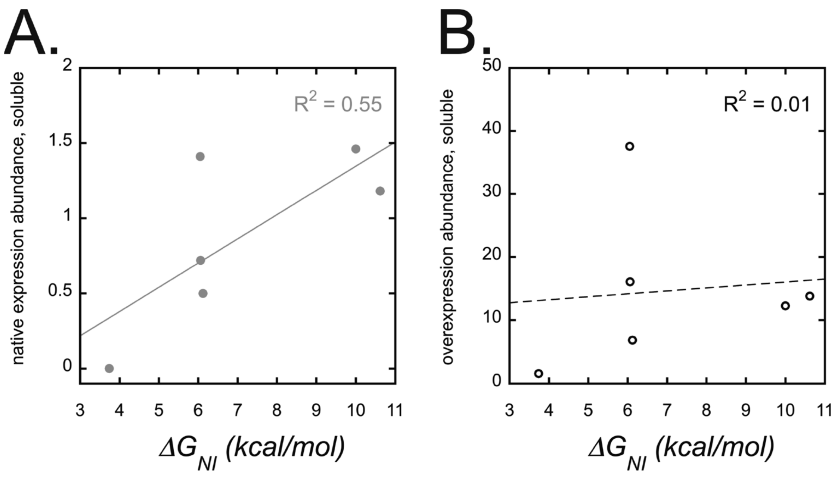

Figure 4. Correlations between abundance and stability in the (A) native expression and (B) overexpression strains. Soluble, periplasmic TEM abundance, as quantified by immunoblotting, has a modest correlation with stability when expression levels are native-like, but no correlation when overexpressed in a strain lacking Lon and OmpT proteases.

soluble G238S is due to increased proteolysis. Indeed, proteolytic susceptibility *in vivo* has been found to inversely correlate with stability[35] because unfolded states are better substrates for proteases. G238S is more likely to unfold than the wild type, causing it to be more efficiently degraded by proteases in the periplasm. If, instead, G238S impacted the maturation process—translocation or removal of the signal sequence—the cytosolic protein would have been detected in the insoluble fraction due to the isolation method used (see the Materials and Methods).

M182T and M182S increase the abundance of both soluble and insoluble fractions, suggesting that aggregation prevention is not a key role in this mutation, as has been previously proposed.[19] Rather, M182T and M182S likely increase soluble protein abundance by protecting against proteolysis, increasing the efficiency of maturation (translocation, signal sequence processing, and folding) or a combination of these strategies. Indeed, a previous work showed that M182T can reduce proteolysis of unstable TEM variants.[36] Our data support a model of proteolytic protection by M182T and M182S since a larger percentage of protein is insoluble in the overexpression strain. These strains are B strain *E. coli*, which lack proteases present in K-12, namely, Lon and OmpT. In the absence of these proteases, partially or totally unfolded proteins may aggregate rather than get degraded as they do in the native expression K-12 strain.

https://doi.org/10.1021/acs.biochem.1c00805
Biochemistry 2022, 61, 398−407

The last observation is that M182T and M182S have similar effects on protein abundance whether alone or in combination with G238S. In the wild-type background, they increase the amount of soluble protein by ∼2−3-fold. When combined with G238S, the effects are even more dramatic, increasing abundance by 10−20-fold. This synergistic effect contrasts with the negative epistasis observed for stability. Because M182T and M182S are not as stabilizing as expected in a G238S background, one might expect that they would not increase abundance as much as in the wild-type background, assuming that abundance correlates with stability. Nonetheless, there is a modest, positive correlation between ΔG_{NI} and abundance of soluble protein (R^2 = 0.55) in the native expression strain (Figure 4A). Interestingly, there is no correlation in the overexpression strain (R^2 = 0.01; Figure 4B), suggesting that in this context, low stability does not lead to greater proteolysis. This may be because this strain is already protease-deficient, and any existing proteases are overwhelmed by the high concentrations of enzyme. The fact that native state stabilities between G238S and the double mutants only differ by ∼2 kcal/mol also demonstrates that even small increases in the intermediate and unfolded populations can result in significantly enhanced proteolysis.

Because intermediate stability is unaffected by the mutations studied, it is not possible to determine whether native state stability relative to the intermediate or unfolded state is more predictive of abundance. For instance, G238S reduces the native population and increases populations of I and U by the same percentage. Still, I represents 0.2% of the G238S population whereas U is only 0.0000002%, so if the intermediate is susceptible to proteolysis, this is likely the dominant route. To test this hypothesis, we performed pulse proteolysis[24] to determine whether the intermediate behaves more like the native or unfolded states in terms of proteolytic susceptibility. In this experiment, samples are equilibrated with varying concentrations of denaturant and then subjected to a brief "pulse" with thermolysin. Samples are separated using SDS-PAGE, and full-length protein is quantified. Unfolded—and potentially partially folded—proteins are degraded during the pulse, so only natively folded protein is detected. Performing this experiment with wild-type TEM, we determined that the partially folded intermediate is degraded along with unfolded protein. This is evident from the striking agreement with fluorescence denaturation, which also tracks the N-to-I transition (Figure 5). Thus, while we cannot entirely rule out the importance of intermediate stability to proteolytic susceptibility, our evidence suggests that unfolding to I is sufficient to result in degradation.

M182T and M182S Do Not Impact Activity. Because abundance is just one component of an enzyme's ability to protect against antibiotics, we next measured the *in vitro* activities of the variants against two antibiotics: benzylpenicillin (BP) and cefotaxime (CFX). Consistent with a previous work,[30] we observe that G238S has a much higher intrinsic catalytic efficiency than wild-type TEM against CFX (100-fold) but slightly lower against BP (3-fold) (Table 3). Although K_ms for CFX cannot be directly compared, since the wild-type enzyme does not exhibit saturation under the conditions tested, G238S's higher activity is likely due to a lower K_m, since it also has a lower K_m for the structurally similar BP. The reaction mechanism proceeds via formation of an acyl-enzyme intermediate, so K_m reflects both affinity of the substrate for the enzyme (K_S) and acylation/deacylation rates.[37] When acylation is rate-limiting, as it is for CFX,[38] K_m approximates K_S, so this reduced K_m suggests enhanced substrate binding by G238S. This would be consistent with the proposed model of G238S pinning down the Ω-loop and stabilizing binding-competent conformations.[26]

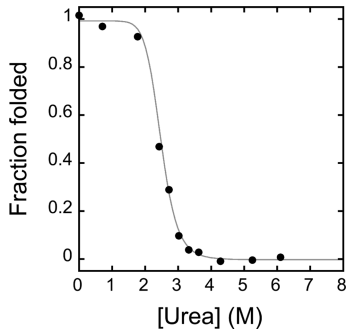

Figure 5. Pulse proteolysis of wild-type TEM (black circles) overlaid with the fit to intrinsic fluorescence denaturation data (gray line). Samples are equilibrated in varying concentrations of urea and treated with thermolysin for a short pulse designed to leave the native state intact. Close agreement with intrinsic fluorescence, which tracks the N-to-I transition, demonstrates that I has similar proteolytic susceptibility to U.

There have been mixed reports in the literature about whether M182T decreases activity slightly or has no effect,[6,13,26] but our data show that there is a modest decrease for both BP and CFX (2-fold). In combination with G238S, the activity more closely resembles G238S than M182T alone with the same reduced K_m and a much higher activity against CFX relative to the wild type. A similar pattern is observed for M182S and G238S/M182S.

Overall, and consistent with previous reports, we find that G238S broadens the substrate specificity by increasing activity against CFX and only slightly reducing activity against BP. Neither M182T nor M182S have much of an impact on activity in either wild-type or G238S backgrounds, so any fitness advantages that they confer are not derived from more efficient catalysis.

M182T and M182S Increase Fitness Only in Combination with G238S. We have shown that M182T and M182S are stabilizing mutations that do not impact the intrinsic activity of TEM, but in what contexts, if any, do they offer fitness advantages? To address this question, we measured fitness using two different approaches: The first determines minimum inhibitory concentrations (MICs) of antibiotics,[39] which is a standard fitness metric for TEM and other resistance mechanisms. The second determines relative fitness based on head-to-head competition assays[40] and is a more versatile and sensitive approach, as explained further below.

MIC data reveal epistasis between G238S and both M182T and M182S, revealing a fitness advantage only when combined. Alone, M182T and M182S resemble the wild type and have no effect on MIC values for either drug, which is mirrored by their shared catalytic constants (Table 3). Interestingly, there are also greater quantities of insoluble protein in M182T and M182S strains, indicating that aggregation is not, in and of itself, detrimental to fitness. The double mutants (M182T/G238S and M182S/G238S), however, exhibit a higher resistance relative to G238S alone despite having similar catalytic constants, likely due to the ability of M182T and M182S to increase abundance (Table 2).

To explore this idea further, we assessed whether catalytic constants and/or abundance were predictive of the measured MIC values. The MIC values for BP correlate better with k_{cat} (R^2

https://doi.org/10.1021/acs.biochem.1c00805
Biochemistry 2022, 61, 398−407

Table 3. *In Vitro* Catalytic Activities of TEM Variants

	benzylpenicillin (BP)			cefotaxime (CFX)		
	k_{cat} (s^{-1})[b]	K_m (μM)[b]	k_{cat}/K_m (μM^{-1} s^{-1})	k_{cat} (s^{-1})[b]	K_m (μM)[b]	k_{cat}/K_m (μM^{-1} s^{-1})
wild-type	1286.2 ± 112.6	51.0 ± 11.9	25.22 ± 6.29	nd[a]	nd[a]	$2.03 \times 10^{-3} \pm 0.05 \times 10^{-3}$
M182T	1107.3 ± 52.5	77.7 ± 8.4	14.25 ± 1.69	nd[a]	nd[a]	$9.48 \times 10^{-4} \pm 0.34 \times 10^{-4}$
M182S	1242.9 ± 47.8	76.3 ± 6.77	16.29 ± 1.57	nd[a]	nd[a]	$8.34 \times 10^{-4} \pm 0.39 \times 10^{-4}$
G238S	72.6 ± 3.2	9.6 ± 2.1	7.59 ± 1.71	49.0 ± 3.5	186.2 ± 22.4	0.26 ± 0.04
M182T/G238S	93.5 ± 1.4	5.6 ± 0.6	16.64 ± 1.68	78.5 ± 3.2	215.0 ± 14.0	0.37 ± 0.03
M182S/G238S	77.4 ± 1.4	7.1 ± 0.7	10.90 ± 1.14	80.9 ± 10.1	315.0 ± 58.0	0.26 ± 0.06

[a]Not determined. k_{cat}/K_m was determined by a linear fit because the saturation behavior was not observed at the highest measurable substrate concentration. [b]Errors are standard errors of the fits to average values of triplicate measurements at each substrate concentration.

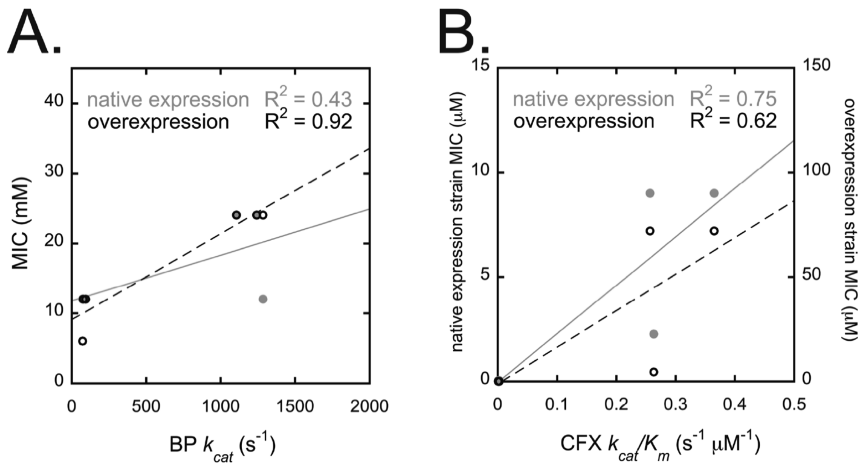

Figure 6. Correlations between *in vitro* activities and MICs for (A) BP and (B) CFX. k_{cat} and k_{cat}/K_m correlate with MICs for BP and CFX, respectively, suggesting that an enzyme's intrinsic activity for its substrate is predictive of its fitness.

Table 4. Relative Fitness of Competing Strains

		relative to the wild type (TEM-1)[b]			relative to G238S[b]	relative to M182T/G238S[b]
amino acid substitution	clinical variant	no drugs	5 mM BP	30 nM CFX	500 nM CFX	1500 nM CFX
M182T	TEM-135	0.97 ± 0.06	0.95 ± 0.07	0.85 ± 0.15	nd[c]	nd[c]
M182S	na[a]	1.00 ± 0.02	0.99 ± 0.08	1.06 ± 0.38	nd[c]	nd[c]
G238S	TEM-19	1.02 ± 0.09	0.66 ± 0.18	2.75 ± 1.14		
M182T/G238S	TEM-20	0.98 ± 0.04	0.99 ± 0.05	1.59 ± 0.12	1.61 ± 0.01	
M182S/G238S	na[a]	1.04 ± 0.06	0.96 ± 0.03	1.84 ± 0.21	1.60 ± 0.02	1.03 ± 0.08

[a]Not applicable. Substitution has not been observed in naturally occurring variants. [b]Errors are standard deviations from triplicate measurements. [c]Not determined.

= 0.43 and R^2 = 0.92, Figure 6A) than k_{cat}/K_m (R^2 = 0.00 and R^2 = 0.50; SI Figure 1). This would make sense if the drug concentrations are well above K_m, meaning the enzymes are saturated and k_{cat} is the relevant rate constant. While this condition is met in the extracellular environment, it has been shown that BP concentrations in the *E. coli* periplasm can be orders of magnitude lower than in the media,[41] making the mechanistic relationship to k_{cat} less clear. Overall, correlations are more pronounced in the overexpression stains, but when differences in abundance are taken into account, the correlation for native expression is improved (R^2 = 0.90; SI Figure 2A).

MIC values for CFX, on the other hand, are well below the K_m, and so we would expect k_{cat}/K_m to be the relevant rate constant. Indeed, there is good correlation between activity and MIC for both native and overexpression strains (R^2 = 0.75 and R^2 = 0.62; Figure 6B). To our surprise, the correlations do not improve when abundance is included (R^2 = 0.72 and R^2 = 0.69; SI Figure 3). Previous studies with a similar set of variants concluded that thermostability does not impact fitness because including stability did not improve their correlations with MIC.[42] We interpret this result with caution, given the limitations of the assay and the small datasets, since it is clear from our data that M182T and M182S improve CFX MIC values relative to G238S alone, and that the likely molecular mechanism is a higher abundance of soluble protein in the periplasm. One explanation is that abundance contributes to fitness only in limited contexts—for instance, when an enzyme has low activity, like for CFX but not BP, or when strains are competing against one another in the same milieu, as in natural populations.

To test whether the fitness advantages conferred by M182T and M182S in G238S-containing strains are altered in more natural contexts, we measured relative fitnesses of strains competing head-to-head in the presence of sublethal drug concentrations. Relative fitness is determined by measuring

https://doi.org/10.1021/acs.biochem.1c00805
Biochemistry 2022, 61, 398−407

growth rates of two or more strains in liquid culture inoculated in equal proportions.[40] The plasmids containing the *bla* genes were modified to include constitutive expression of either mCherry, which fluoresces red, or a non-fluorescence variant of mCherry containing the Y72L substitution.[25] Two variants were competed at a time—one harboring the fluorescent mCherry and one with the non-fluorescent variant. Samples from the co-culture were plated and resulting colonies counted after mixing ($t = 0$) and at later time points to determine the relative growth rates, used here to represent their relative fitness, W_{ij}:

$$W_{ij} = \frac{\ln\left(\frac{N_{i,final}}{N_{i,initial}}\right)}{\ln\left(\frac{N_{j,final}}{N_{j,initial}}\right)} \quad (3)$$

where $N_{initial}$ is the number of colony-forming units at $t = 0$ and N_{final} is the number at the final time point.

In the absence of antibiotics and in the presence of sublethal concentrations of BP, all strains have the same fitness as the wild type (Table 4). The concentration of BP used, 5 mM, is comparable or slightly higher than concentrations in the sera of patients treated for infection,[43] which means that in clinical settings, these variants have no selective advantage or disadvantage. In the presence of 30 nM CFX, G238S-containing strains are about twice as fit as the wild type but similar to one another. This is, perhaps, less of a difference than might be expected given their MICs, which indicate that G238S-containing strains have CFX MICs that are 50−100 times higher than the wild type. This highlights one difference between the methods of fitness determination and suggests that MICs represent an upper bound of strain fitness since they do not account for mixed culture conditions where strains can directly impact one another. For instance, because TEM is exported to the periplasm, it is likely that the enzyme produced by one cell offers some protection to its neighbors by removing excess drug from the local environment, as would occur in natural settings. This would explain why in isolation G238S appears to offer a much larger fitness advantage over the wild type than when they are cultured together. Competitions in the presence of more physiological concentrations of cefotaxime were not possible since all the strains' MICs are well below concentrations found in treated patient sera (~450 mM)[44] even as they meet the CLSI definition for cefotaxime resistance (8 mM).[45] However, at the highest concentrations tested, the double mutants were 1.6 times more fit than G238S with no fitness differences between the double mutants.

Taken together, the fitness data reveal that M182T and M182S interact with G238S to increase resistance against CFX but not BP. In the background of the wild type, however, M182T and M182S have no measurable impact on fitness. Because these mutations impact stability but not activity, it is likely that stability effects are the source of epistasis. We observe that stability correlates with abundance in the cell—with less stable proteins like G238S being more prone to proteolysis rather than aggregation—and the higher enzyme concentrations enable greater resistance and faster growth rates.

M182S Will Evolve under Neutral Drift. By all metrics, M182S is indistinguishable from M182T. *In vitro* activities and stabilities are the same whether in the wild-type or G238S backgrounds. Also, *in vivo*, there are no detectable differences in fitness under any conditions tested. From a protein perspective, there is every reason to expect that this mutation is adaptive and should exist in natural populations. Or, taken another way, its absence from natural populations does not indicate that it is *not* adaptive. So why is it that M182S has not (yet) been observed clinically?

If we take a step back and look at the larger family of structurally related β-lactamases (specifically subclass A1[46]), TEM appears to be the exception rather than the rule: Thr at position 182 is the ancestral state and Met is present only in the TEM lineage.[47] Ser is observed in certain derived lineages, too, further highlighting the degeneracy of Ser and Thr at this position. From this perspective, the more salient question may be why TEM lost Thr rather than why it reacquires it under high selective pressure.

As our data definitively demonstrate, the most consequential difference between M182T and M182S is not the effect of the amino acid substitution on the protein's properties but in the genetic accessibility of the mutation. A single nucleotide change is sufficient for M182T (ATG → ACG), whereas two changes are required for M182S. Two substitutions at this locus in a single generation are very unlikely, and so Thr is the more probable substitution, assuming that you start from the wild-type Met codon.

However, positive selection is only one way that mutations can get fixed in a population. More commonly, fixation occurs under neutral drift conditions, albeit far more slowly than when under selection, with a probability of fixation equal to the mutation rate.[48] Because M182S is a neutral change relative to M182T, and only one nucleotide substitution is required to change from Thr to Ser (ACG → TCG, for example), we can calculate the time until fixation, assuming that you start with the Thr codon:

$$\text{time}_{\text{fixation of a specific neutral mutation}} = \frac{1}{\text{mutation rate} \times \text{generation time}} \quad (4)$$

For bacteria, mutation rates are typically cited as 10^{-7} to 10^{-9} but can be 10−100-fold higher under high selective pressures.[49,50] Using eq 4 and assuming 10^{-7} errors per base pair per generation and 20 min per division, you would expect fixation of a given mutation to occur in 380 years. It is reasonable to assume that although TEM predates human antibiotic usage, M182T has increased in prevalence more recently due to human use of β-lactam antibiotics and inhibitors. Widespread use of β-lactam antibiotics developed in the 1950s,[51] so there has been ~70 years of opportunity for neutral drift to drive change from Thr to Ser at position 182. Simply put, there has not been enough time to observe fixation of M182S under neutral drift conditions. However, because mutation rates in bacteria are highly variable—and can be particularly high in pathogenic strains[50]—we might expect to observe M182S in clinical isolates in as little as 38 years (with a 10^{-6} mutation rate). Thus, it is possible that this substitution might yet appear.

CONCLUSIONS

The ability to predict the impact of missense mutations on fitness—and to anticipate adaptive mutations before they arise—is a central goal in molecular genetics. Here, we demonstrate that adopting a protein-centric view can only get you so far. Coupling *in vitro* characterization of protein activity and stability with quantitative measurements of fitness, we have determined that the synthetic mutation M182S is no different from the naturally occurring M182T. Both share the same

https://doi.org/10.1021/acs.biochem.1c00805
Biochemistry 2022, 61, 398−407

catalytic activity as the wild-type enzyme, stabilize the native state, and suppress proteolysis, leading to a higher abundance of both soluble and insoluble enzymes. The fact that two nucleotide substitutions are required to acquire M182S makes it less accessible at the genetic level, but given enough time, we predict this mutation will also arise in natural populations under neutral drift. We also discovered lessons about how stability and activity of enzymes involved in antibiotic resistance can contribute to fitness: first, intrinsic activity is the main parameter underlying fitness of naturally occurring variants. Any variant with prohibitively low stability will be purged from the population, so any naturally occurring variant is stable enough. This suggests the threshold behavior—anything over a critical value is sufficient—rather than fitness tracking with stability over a broad range. Second, genetic context matters. We found that a higher stability was more important when the enzyme was not overexpressed and that this effect was likely mediated by the presence of proteases. Last, aggregation in and of itself does not necessarily exact a fitness cost. In this case, the presence of partially and fully unfolded states is problematic due to loss-of-function rather than gain-of-function toxicity from aggregates. Since intermediates are more prevalent than unfolded states, it is important to consider their accessibility when exploring how stability constrains protein evolution and evolvability.

■ ASSOCIATED CONTENT

Supporting Information

The Supporting Information is available free of charge at https://pubs.acs.org/doi/10.1021/acs.biochem.1c00805.

Additional correlation plot figures (PDF)

Accession Codes

UniProt accession ID: P62593 (BLAT_ECOLX).

■ AUTHOR INFORMATION

Corresponding Author

Kathryn M. Hart − *Department of Chemistry, Williams College, Williamstown, Massachusetts 01267, United States;* orcid.org/0000-0002-5277-8872; Email: kmh8@williams.edu

Authors

Sonya Lee − *Department of Chemistry, Williams College, Williamstown, Massachusetts 01267, United States*

Cynthia N. Okoye − *Department of Chemistry, Williams College, Williamstown, Massachusetts 01267, United States;* Present Address: Department of Pharmacology, University of Cambridge, Cambridge, Tennis Court Road, Cambridge CB2 1PD, United Kingdom

Devin Biesbrock − *Department of Chemistry, Williams College, Williamstown, Massachusetts 01267, United States*

Emily C. Harris − *Department of Chemistry, Williams College, Williamstown, Massachusetts 01267, United States*

Katelyn F. Miyasaki − *Department of Biochemistry & Molecular Biophysics, Washington University School of Medicine, St. Louis, Missouri 63110, United States;* Present Address: Department of Bioengineering, University of California San Diego, 9500 Gilman Drive, La Jolla, California 92093, United States

Ryan G. Rilinger − *Department of Chemistry, Williams College, Williamstown, Massachusetts 01267, United States;* Present Address: Beth Israel Deaconess Medical Center, 330 Brookline Avenue, Boston, Massachusetts 02215, United States

Megalan Tso − *Department of Chemistry, Williams College, Williamstown, Massachusetts 01267, United States*

Complete contact information is available at: https://pubs.acs.org/10.1021/acs.biochem.1c00805

Author Contributions

#S.L. and C.N.O. contributed equally to this work. K.M.H. conceived the work, collected and analyzed the data, and wrote the manuscript. S.L. and C.N.O. designed the experiments and collected and analyzed the data. K.F.M. constructed the plasmids and collected and analyzed the data. D.B., E.C.H., R.G.R., and M.T. collected and analyzed the data. All authors reviewed the manuscript.

Notes

The authors declare no competing financial interest.

■ ACKNOWLEDGMENTS

This work was funded by the National Institute of General Medical Sciences of the National Institutes of Health under Award Number R15GM135639. The content is solely the responsibility of the authors and does not necessarily represent the official views of the National Institutes of Health. We thank Katie Tripp, Amy Gehring, and Nate Cook for helpful comments on the manuscript.

■ REFERENCES

(1) Clemente, J. C.; Pehrsson, E. C.; Blaser, M. J.; Sandhu, K.; Gao, Z.; Wang, B.; Magris, M.; Hidalgo, G.; Contreras, M.; Noya-Alarcón, O.; Lander, O.; McDonald, J.; Cox, M.; Walter, J.; Oh, P. L.; Ruiz, J. F.; Rodriguez, S.; Shen, N.; Song, S. J.; Metcalf, J.; Knight, R.; Dantas, G.; Dominguez-Bello, M. G. The microbiome of uncontacted Amerindians. *Sci. Adv.* **2015**, *1*, No. e1500183.

(2) Medeiros, A. A. Evolution and Dissemination of β-Lactamases Accelerated by Generations of β-Lactam Antibiotics. *Clin. Infect. Dis.* **1997**, *24*, S19−S45.

(3) Hall, B. G. Predicting evolution by in vitro evolution requires determining evolutionary pathways. *Antimicrob. Agents Chemother.* **2002**, *46*, 3035−3038.

(4) Naas, T.; Oueslati, S.; Bonnin, R. A.; Dabos, M. L.; Zavala, A.; Dortet, L.; Retailleau, P.; Iorga, B. I. Beta-lactamase database (BLDB) − structure and function. *J. Enzyme Inhib. Med. Chem.* **2017**, *32*, 917−919.

(5) Orencia, M. C.; Yoon, J. S.; Ness, J. E.; Stemmer, W. P. C.; Stevens, R. C. *Predicting the emergence of antibiotic resistance by directed evolution and structural analysis.* http://structbio.nature.com (2001).

(6) Wang, X.; Minasov, G.; Shoichet, B. K. Evolution of an Antibiotic Resistance Enzyme Constrained by Stability and Activity Trade-offs. *J. Mol. Biol.* **2002**, *320*, 85−95.

(7) Meiering, E. M.; Serrano, L.; Fersht, A. R. Effect of active site residues in barnase on activity and stability. *J. Mol. Biol.* **1992**, *225*, 585−589.

(8) Shoichet, B. K.; Baase, W. A.; Kuroki, R.; Matthews, B. W. A relationship between protein stability and protein function. *Proc. Natl. Acad. Sci. U. S. A.* **1995**, *92*, 452−456.

(9) Tokuriki, N.; Tawfik, D. S. Stability effects of mutations and protein evolvability. *Curr. Opin. Struct. Biol.* **2009**, *19*, 596−604.

(10) Bloom, J. D.; Wilke, C. O.; Arnold, F. H.; Adami, C. Stability and the evolvability of function in a model protein. *Biophys. J.* **2004**, *86*, 2758−2764.

(11) Gong, L. I.; Suchard, M. A.; Bloom, J. D. Stability-mediated epistasis constrains the evolution of an influenza protein. *eLife* **2013**, *2*, No. e00631.

(12) Bloom, J. D.; Labthavikul, S. T.; Otey, C. R.; Arnold, F. H. Protein stability promotes evolvability. *Proc. Natl. Acad. Sci. U. S. A.* **2006**, *103*, 5869−5874.
(13) Dobson, C. M. Protein folding and misfolding. *Nature* **2003**, *426*, 884−890.
(14) Bucciantini, M.; Giannoni, E.; Chiti, F.; Baroni, F.; Formigli, L.; Zurdo, J.; Taddei, N.; Ramponi, G.; Dobson, C. M.; Stefani, M. Inherent toxicity of aggregates implies a common mechanism for protein misfolding diseases. *Nature* **2002**, *416*, 507−511.
(15) Connell, K. B.; Miller, E. J.; Marqusee, S. The Folding Trajectory of RNase H Is Dominated by Its Topology and Not Local Stability: A Protein Engineering Study of Variants that Fold via Two-State and Three-State Mechanisms. *J. Mol. Biol.* **2009**, *391*, 450−460.
(16) Spudich, G. M.; Miller, E. J.; Marqusee, S. Destabilization of the Escherichia coli RNase H Kinetic Intermediate: Switching Between a Two-state and Three-state Folding Mechanism. *J. Mol. Biol.* **2004**, *335*, 609−618.
(17) Kachlishvili, K.; Dave, K.; Gruebele, M.; Scheraga, H. A.; Maisuradze, G. G. Eliminating a Protein Folding Intermediate by Tuning a Local Hydrophobic Contact. *J. Phys. Chem. B* **2017**, *121*, 3276−3284.
(18) Mogensen, J. E.; Ipsen, H.; Holm, J.; Otzen, D. E. Elimination of a Misfolded Folding Intermediate by a Single Point Mutation. *Biochemistry* **2004**, *43*, 3357−3367.
(19) Sideraki, V.; Huang, W.; Palzkill, T.; Gilbert, H. F. A secondary drug resistance mutation of TEM-1 β-lactamase that suppresses misfolding and aggregation. *Proc. Natl. Acad. Sci. U. S. A.* **2001**, *98*, 283−288.
(20) Zimmerman, M. I.; Hart, K. M.; Sibbald, C. A.; Frederick, T. E.; Jimah, J. R.; Knoverek, C. R.; Tolia, N. H.; Bowman, G. R. Prediction of New Stabilizing Mutations Based on Mechanistic Insights from Markov State Models. *ACS Cent. Sci.* **2017**, *3*, 1311−1321.
(21) Ghrayeb, J.; Kimura, H.; Hsiung, M. T.; Masui, Y.; Inouye, M. Secretion cloning vectors in Escherichia coli. *EMBO J.* **1984**, *3*, 2437−2442.
(22) Pace, C. N.; Vajdos, F.; Fee, L.; Grimsley, G.; Gray, T. How to measure and predict the molar absorption coefficient of a protein. *Protein Sci* **1995**, *4*, 2411−2423.
(23) Santoro, M. M.; Bolen, D. W. Unfolding free energy changes determined by the linear extrapolation method. 1. Unfolding of phenylmethanesulfonyl .alpha.-chymotrypsin using different denaturants. *Biochemistry* **1988**, *27*, 8063−8068.
(24) Park, C.; Marqusee, S. Quantitative Determination of Protein Stability and Ligand Binding by Pulse Proteolysis. *Curr. Protoc. Protein Sci.* **2006**, *46*, 20.11.1−20.11.14.
(25) Yamashita, S.; Tsuboi, T.; Ishinabe, N.; Kitaguchi, T.; Michiue, T. Wide and high resolution tension measurement using FRET in embryo. *Sci. Rep.* **2016**, *6*, 28535.
(26) Hart, K. M.; Ho, C. M. W.; Dutta, S.; Gross, M. L.; Bowman, G. R. Modelling proteins' hidden conformations to predict antibiotic resistance. *Nat. Commun.* **2016**, *7*, 12965.
(27) Dagan, S.; Hagai, T.; Gavrilov, Y.; Kapon, R.; Levy, Y.; Reich, Z. Stabilization of a protein conferred by an increase in folded state entropy. *Proc. Natl. Acad. Sci.* **2013**, *110*, 10628.
(28) Matthews, B. W.; Nicholson, H.; Becktel, W. J. Enhanced protein thermostability from site-directed mutations that decrease the entropy of unfolding. *Proc. Natl. Acad. Sci. U. S. A.* **1987**, *84*, 6663−6667.
(29) Shcherbinin, D.; Veselovsky, A.; Rubtsova, M.; Grigorenko, V.; Egorov, A. The impact of long-distance mutations on the Ω-loop conformation in TEM type β-lactamases. *J. Biomol. Struct. Dyn.* **2020**, *38*, 2369−2376.
(30) Palzkill, T. Structural and mechanistic basis for extended-spectrum drug-resistance mutations in altering the specificity of TEM, CTX-M, and KPC β-lactamases. *Front. Mol. Biosci.* **2018**, *5*, 16.
(31) Roggenkamp, R.; Dargatz, H.; Hollenberg, C. P. Precursor of beta-lactamase is enzymatically inactive. Accumulation of the preprotein in Saccharomyces cerevisiae. *J. Biol. Chem.* **1985**, *260*, 1508−1512.
(32) So, M.; Gill, R.; Falkow, S. The generation of a ColE1-Apr cloning vehicle which allows detection of inserted DNA. *Mol. Gen. Genet. MGG* **1975**, *142*, 239−249.
(33) Bolivar, F.; Rodriguez, R. L.; Greene, P. J.; Betlach, M. C.; Heyneker, H. L.; Boyer, H. W.; Crosa, J.; Falkow, S. Construction and characterization of new cloning vehicles. II. A multipurpose cloning system. *Gene* **1977**, *2*, 95−113.
(34) Georgiou, G.; Telford, J. N.; Shuler, M. L.; Wilson, D. B. Localization of inclusion bodies in Escherichia coli overproducing beta-lactamase or alkaline phosphatase. *Appl. Environ. Microbiol.* **1986**, *52*, 1157−1161.
(35) Parsell, D. A.; Sauer, R. T. The structural stability of a protein is an important determinant of its proteolytic susceptibility in Escherichia coli. *J. Biol. Chem.* **1989**, *264*, 7590−7595.
(36) Huang, W.; Palzkill, T. A natural polymorphism in β-lactamase is a global suppressor. *Proc. Natl. Acad. Sci. U. S. A.* **1997**, *94*, 8801−8806.
(37) Raquet, X.; Lamotte-Brasseur, J.; Fonze, E.; Goussard, S.; Courvalin, P.; Frere, J. M. TEM β-Lactamase Mutants Hydrolysing Third-generation Cephalosporins: A Kinetic and Molecular Modelling Analysis. *J. Mol. Biol.* **1994**, *244*, 625−639.
(38) Saves, I.; Burlet-Schlitz, O.; Maveyraud, L.; Samama, J. P.; Prome, J. C.; Masson, J. M. Mass Spectral Kinetic Study of Acylation and Deacylation During the Hydrolysis of Penicillins and Cefotaxime by .beta.-Lactamase TEM-1 and the G238S Mutant. *Biochemistry* **1995**, *34*, 11660−11667.
(39) Jorgensen, J. H. Methods for dilution antimicrobial susceptibility tests for bacteria that grow aerobically: approved standard. *National Committee for Clinical Laboratory Standards Antimicrobial Susceptibility Testing*; NCCLS document M7-A3. (1993).
(40) Lenski, R. E.; Rose, M. R.; Simpson, S. C.; Tadler, S. C. Long-Term Experimental Evolution in Escherichia coli. I. Adaptation and Divergence During 2,000 Generations. *Am. Nat.* **1991**, *138*, 1315−1341.
(41) Kojima, S.; Nikaido, H. Permeation rates of penicillins indicate that Escherichia coli porins function principally as nonspecific channels. *Proc. Natl. Acad. Sci. U. S. A.* **2013**, *110*, E2629−E2634.
(42) Knies, J. L.; Cai, F.; Weinreich, D. M. Enzyme Efficiency but Not Thermostability Drives Cefotaxime Resistance Evolution in TEM-1 β-Lactamase. *Mol. Biol. Evol.* **2017**, *34*, 1040−1054.
(43) Sandoz, A *Novartis Division. Penicillin G Sodium for Injection*; U.S. Food and Drug Administration https://www.accessdata.fda.gov/drugsatfda_docs/label/2012/065068s013lbl.pdf (2021).
(44) *Baxter Healthcare Corporation for sanofi-aventis U.S. LLC. Claforan Sterile (cefotaxime for injection)*; U.S. Food and Drug Administration https://www.accessdata.fda.gov/drugsatfda_docs/label/2015/050547s071,050596s042lbl.pdf (2021).
(45) Clinical and Laboratory Standards Institute. *Performance standards for antimicrobial susceptibility testing*; 31st edition; CLSI document M100-ED31. (2021).
(46) Philippon, A.; Slama, P.; Dény, P.; Labia, R. A Structure-Based Classification of Class A β-Lactamases, a Broadly Diverse Family of Enzymes. *Clin. Microbiol. Rev.* **2016**, *29*, 29−57.
(47) Risso, V. A.; Gavira, J. A.; Mejia-Carmona, D. F.; Gaucher, E. A.; Sanchez-Ruiz, J. M. Hyperstability and substrate promiscuity in laboratory resurrections of Precambrian β-lactamases. *J. Am. Chem. Soc.* **2013**, *135*, 2899−2902.
(48) Kimura, M. Evolutionary Rate at the Molecular Level. *Nature* **1968**, *217*, 624−626.
(49) Westra, E. R.; Sünderhauf, D.; Landsberger, M.; Buckling, A. Mechanisms and consequences of diversity-generating immune strategies. *Nat. Rev. Immunol.* **2017**, *17*, 719−728.
(50) Matic, I.; Radman, M.; Taddei, F.; Picard, B.; Doit, C.; Bingen, E.; Denamur, E.; Elion, J. Highly variable mutation rates in commensal and pathogenic Escherichia coli. *Science* **1997**, *277*, 1833−1834.
(51) Bush, K.; Bradford, P. A. β-Lactams and β-Lactamase Inhibitors: An Overview. *Cold Spring Harbor Perspect. Med.* **2016**, *6*, a025247.

https://doi.org/10.1021/acs.biochem.1c00805
Biochemistry 2022, 61, 398−407